Available online at www.sciencedirect.com
SCIENCE DIRECT®
Tectonophysics 376 (2003) 99–115
TECTONOPHYSICS
www.elsevier.com/locate/tecto

Analogue modeling of overlapping spreading centers: insights into their propagation and coalescence

Tatiana Tentler*

Hans Ramberg Tectonic Laboratory, Department of Earth Sciences, Uppsala University, Villavagen 16, Uppsala, SE-75236 Sweden

Received 11 December 2002; accepted 25 August 2003

Abstract

The propagation and segmentation of mid-ocean ridges is studied using centrifuged analogue models built with non-linear materials. The deformation of the brittle-ductile model is controlled by diapiric uprise of buoyant analogous asthenospheric material induced by a centrifugal body force. This linear upwelling laterally stretches the model mantle that, in turn, induces failure in the upper layer simulating the brittle crust. Arrays of fractures initiate within zones of high stress concentration above the diapir. Fractures propagate laterally in a direction perpendicular to the maximum tensile (the minimum principal) stress. Secondary tension cracks initiate in the vicinity of parent fracture tips. Through-going fractures that crosscut the model surface develop by short fractures propagating toward each other and coalescing in different types of patterns. The overlap, overstep and inclination of fractures developed at the initial stage of extension control their subsequent growth and coalescence. Non-overlapping sub-parallel fractures propagate along nearly straight paths and coalesce to produce a single planar fracture. If overlapping fractures are parallel, they propagate towards each other along curved paths that enclose an intervening elliptical core of intact material. Fracture curvature in this case results from crack–crack interaction and is similar to that of overlapping spreading centers (OSCs) observed along mid-ocean ridges. Overlapping non-parallel fractures tend to coalesce by one of their tips propagating sub-parallel to the spreading direction toward the other fracture. Such offsets can serve as models for the development of the orthogonal ridge-transform fault patterns common along mid-ocean ridges.

Keywords: Mid-ocean ridge; Fracture; Segments; Overlapping spreading centers; Analogue modeling

1. Introduction

1.1. Purpose

Extension across mid-ocean ridges is commonly accommodated by normal faulting at crustal depths between a few hundred meters and a few kilometers and by both normal faults and vertical tension fractures at shallower depths (Lonsdale, 1983; Macdonald et al., 1984; Macdonald, 1986; Shaw and Lin, 1993; Angelier et al., 1997; Krasnov et al., 1997; Gudmundsson, 2000). Extensional structures at spreading ridges occur within 10 km of their axis and tend to strike perpendicular to the lowest principal compressive stress and therefore the spreading direction (Macdonald, 1998). Extension of the crust due to normal faulting is estimated as 10–20% across slow-spreading ridges and 3–5% across fast-spreading

* Fax: +46-18-471-2591.
E-mail address: tatiana.tentler@geo.uu.se (T. Tentler).

0040-1951/$ - see front matter © 2003 Elsevier B.V. All rights reserved.
doi:10.1016/j.tecto.2003.08.011

ridges (Cowie et al., 1993; Solomon et al., 1988; Macdonald, 1998). The maximum fault scarp height can exceed 1 km along slow-spreading centers, but rarely exceeds a few hundred meters along fast-spreading centers (Cowie, 1998). The linear geometries of axes of spreading centers contribute to linkage of co-linear normal faults and tensional fractures resulting in long ridge-parallel structures (McAlister and Cann, 1996).

The present paper studies fracture growth in a tensile stress field by means of centrifuge modeling using analogue materials. Each dilational fracture in the brittle upper layer of a model represents a segment of a spreading ridge on the ocean floor. Analyses of the interaction of fractures on the surface of the models allows inferences about the propagation and linkage of segments of oceanic spreading ridges. The analogy between ocean ridge segments and extensional fractures was first emphasized by Shih and Molnar, (1975) while using magnetic anomalies data to investigate spreading centers and by Oldenburg and Brune (1975) while discussing analogue models of orthogonal ridge-transform patterns. The analogy has been corroborated by a number of other analogue (Macdonald et al., 1984; Shemenda and Grocholsky, 1991, 1994) and numerical model studies (Pollard and Aydin, 1984; De Bremaecker and Swenson, 1990; Gudmundsson, 1993; Gudmundsson and Homberg, 1999). All these studies have justified the argument that the distribution of stress in an extending fractured brittle layer approximates that induced by complex of ridge processes on the ocean floor.

Centrifuge modeling uses centrifugal force to scale the action of gravity in driving deformation. In the present experiments, rotation of the models in a centrifuge causes upwelling of a viscous buoyant material simulating the asthenosphere. This diapiric upwelling results in the nucleation and propagation of fractures in the brittle upper layer simulating ridge segments. Despite extensive studies of the processes of mid-ocean ridge propagation, many aspects of ridge development are still not understood, particularly how the location and orientation of spreading centers relate to configuration of overlap zones and how transform zones develop. The model results allow inferences concerning such interaction of oceanic ridge segments.

1.2. Previous work

Previous work has shown that the direction of fracture propagation in a homogeneous isotropic medium depends upon the remote stress field (Jaeger and Cook, 1979) interacting with stress fields around the tips of existing fractures (Lawn and Wilshaw, 1975). The paths along which fracture tips propagate are likely to be planar in a compressive stress field and deflected away from the planar in fracture-parallel tension (Cotterell and Rice, 1980). Pollard and Aydin (1984) investigated the propagation of spreading ridge segments and the structures that link them using cracks in elastic plates as analogs. In their model, hook-shaped cracks form where the ends of two adjacent ridges approach each other and overlap. They demonstrated the effect of the initial crack length and offset on the interaction of straight en echelon cracks. Sempere and Macdonald (1986) numerically modeled the coalescence of two parallel elastic cracks and showed that the initial crack offset is inversely proportional to both the elongation of the overlap region and the degree that cracks deviate from each other before curving inward.

Olson and Pollard (1989) investigated the relation between fracture paths and state of stress. They found that a small compressive stress eliminates the divergence of crack-paths and reduces their convergence, while higher compressive stress produces nearly planar paths. In contrast, tensile stress exaggerates path curvature, so that propagating fractures approach neighboring crack planes at an angle that is nearly perpendicular. Olson (1993) examined the generation of fracture networks using a model of fracture mechanics that tracks the propagation of cracks. He concluded that it is the fracture propagation velocity that controls their length distribution and spacing. Tuckwell et al. (1998) employed boundary element modeling to simulate the propagation and linkage of a large number of fractures in a two-dimensional infinite elastic medium. Fracture growth in their model occurred by iteration between processes of propagation, tip-to-tip linkage and tip-to-wall linkage as fracture tips propagated towards neighboring fractures.

Oldenburg and Brune (1975) used wax models to show that the parameter that characterizes the ability of a wax to generate the orthogonal ridge-transform fault pattern characteristic of oceanic ridges is the ratio of the shear strength of the solid wax to the

resistive stresses acting along the transform. Thomas and Pollard (1993) showed how the curvature of echelon fractures depends on the fracture spacing and magnitude of the remote differential stress. In their thermo-mechanical model of seafloor spreading, Shemenda and Grocholsky (1994) generated transfer zones between propagating ridge segments by inducing the jump of the spreading centers when horizontal tension and vertical non-isostatic forces were applied. Uniaxial compression experiments by Shen et al. (1995) suggest that the coalescence mechanism of two pre-existing fractures depends on the angle of inclination of the rock bridge between pre-existing fractures. Modeling by Dauteuil and Mart (1998) provided a better understanding of the deep structures that develop in transform zones between mid-ocean ridge segments and their superficial expressions.

This paper takes into account the results of previous modeling and aims to study how spreading ridges interact. Analogue models at different stages of deformation are compared to infer how the initial geometry of ridges modeled as dilational fractures controls their growth and subsequent coalescence as extension progresses.

2. Analogue materials

Analogue tectonic experiments under normal gravity or in a centrifuge require model materials that deform at time and space scales convenient for replicating natural geological processes (Ramberg, 1981; Weijermars and Schmeling, 1986). The models described here consisted of specially prepared materials that do not display Newtonian viscous behavior where stress and strain rate have a linear relationship. Instead, at the strain rates involved during deformation of the models, these materials obey a power law with respect to the induced stresses and the deformation. Such mechanical properties in the experiments closely resemble the deformation of rocks in nature (Ranalli, 1987; Goodman, 1989; Davies, 1999). A strain-softening material was used to simulate the brittle crust. This was prepared as a homogenized mixture of: 40 wt.% paraffin wax, 35 wt.% Vaseline and 25 wt.% plaster of Paris, which was heated, stirred when molten and then cooled. To represent the lithospheric mantle and the asthenosphere, materials of non-linear rheology with power law exponents between 1.3 and 4.0 were prepared as mixtures of industrially manufactured silicone polymer (Rhodorsil Gomme) and painter's putty. A mixture of density 1.05×10^3 kg m^{-3} and viscosity of 3×10^4 Pa s was chosen as an analogue for the upper asthenosphere and a putty mixture of density 1.20×10^3 kg m^{-3} and viscosity of 7.25×10^5 Pa s was used to simulate the lithospheric mantle. The physical properties measured as described by Tentler (2001) for each analogue material and the thickness of each layer used in the model are listed in Table 1 where they are compared to the equivalent properties of the natural rocks they represent together with the dynamic scaling ratios. Natural values of key parameters for each model layer (thickness, density, viscosity and strength) are derived from a wide range of geophysical data (Ranalli, 1987; Fowler, 1990). The values of any one parameter for the model materials were adjusted until the dynamic scale ratio was the same for each layer. Thus, the strength of the analogue brittle crust is scaled to the buoyancy stress so that the ratio of stress/strength in the model corresponds to that in nature.

Table 1
Characteristics of analogue materials and model ratios used in the experiments

Earth unit	Thickness	Density (kg m^{-3})	Viscosity (Pa s)	Strength (Pa)
Brittle crust				
Nature	2 km	2.7×10^3		10^7
Model	1 mm	1.05×10^3		1.5×10^4
Model ratio	5×10^{-7}	0.39		1.5×10^{-3}
Mantle				
Nature	80 km	3.00×10^3	10^{21}	
Model	40 mm	1.20×10^3	7.25×10^5	
Model ratio	5×10^{-7}	0.4	7.25×10^{-16}	
Asthenosphere				
Nature	20 km	2.90×10^3	4×10^{19}	
Model	10 mm	1.05×10^3	3×10^4	
Model ratio	5×10^{-7}	0.36	7.5×10^{-16}	

Model ratio is taken as ratio: parameter in model/parameter in nature.

3. Modeling procedure

Models were deformed at the Hans Ramberg Tectonic Laboratory in the large capacity centri-

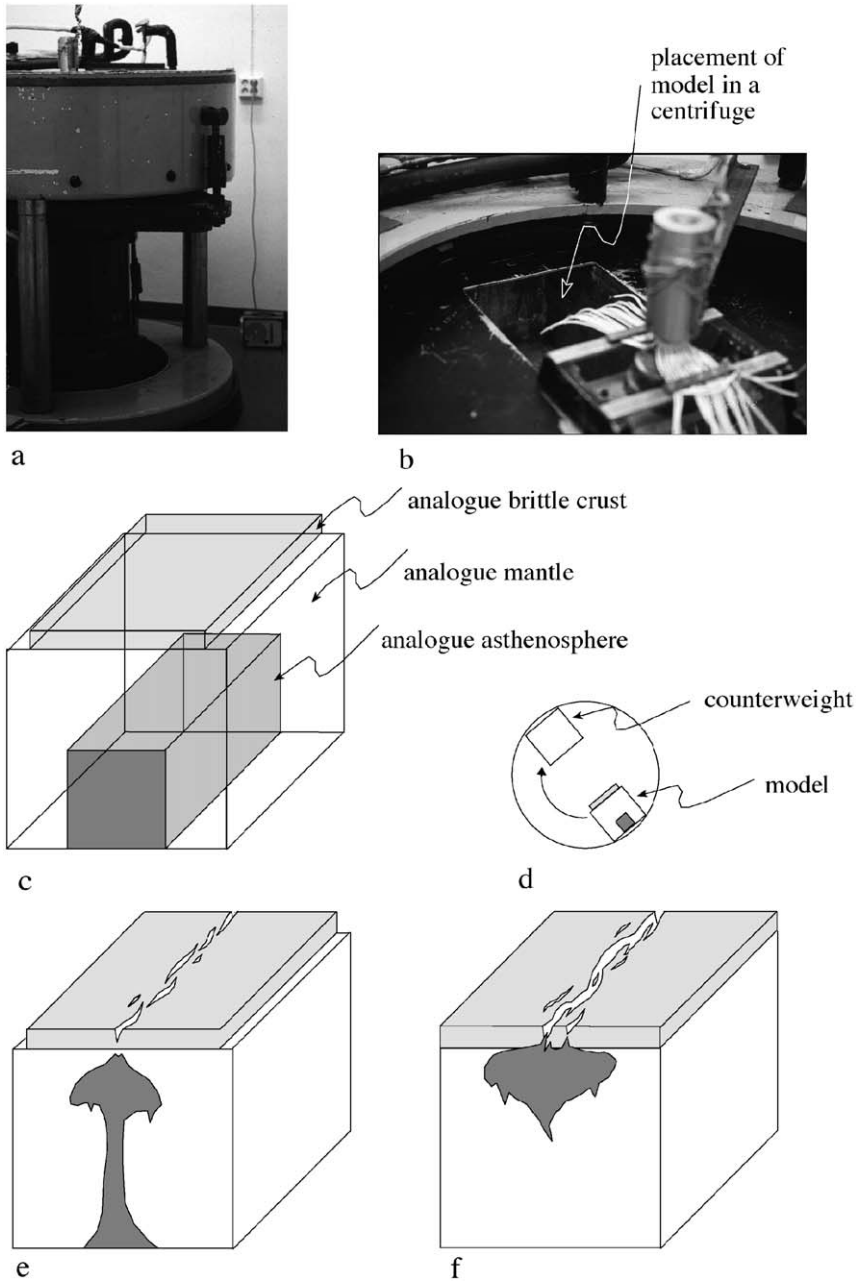

Fig. 1. Experimental apparatus, model design and successive stages of deformation in a centrifuge. (a) Photograph of the centrifuge in the Hans Ramberg Tectonic Laboratory used for the present experiments. (b) View of the centrifuge from the top with a position for model box indicated (counterweight is out of sight in foreground). (c) Model construction. Parallelepiped of the weaker buoyant material imitating the asthenosphere is embedded in a matrix of stiffer material of analogue mantle. Plane layer of semi-brittle material simulating brittle crust is placed on the top. (d) Sketch illustrating rotation of model and counterweight in a centrifuge. (e) Uplift of buoyant material simulating rise of asthenosphere induced by a centrifugal body force. Stretching flow of analogue lithospheric mantle and fracturing of brittle crust. (f) Further fracturing of brittle crust as diapir spreads laterally beneath its surface.

fuge (Fig. 1a,b) described previously by Ramberg (1981) and Mulugeta (1988). Deformation in the experiments described here was driven solely by a centrifugal body force scaled to simulate gravity. Deformation within the models can be interpreted by comparing the distribution of strain on their top surface with that on a series of cut profiles.

The design and general evolution of the models is shown in Fig. 1c–f. For each experiment, two rectangular parallelepipeds of different size were prepared from the mixture of silicone polymer and painter's

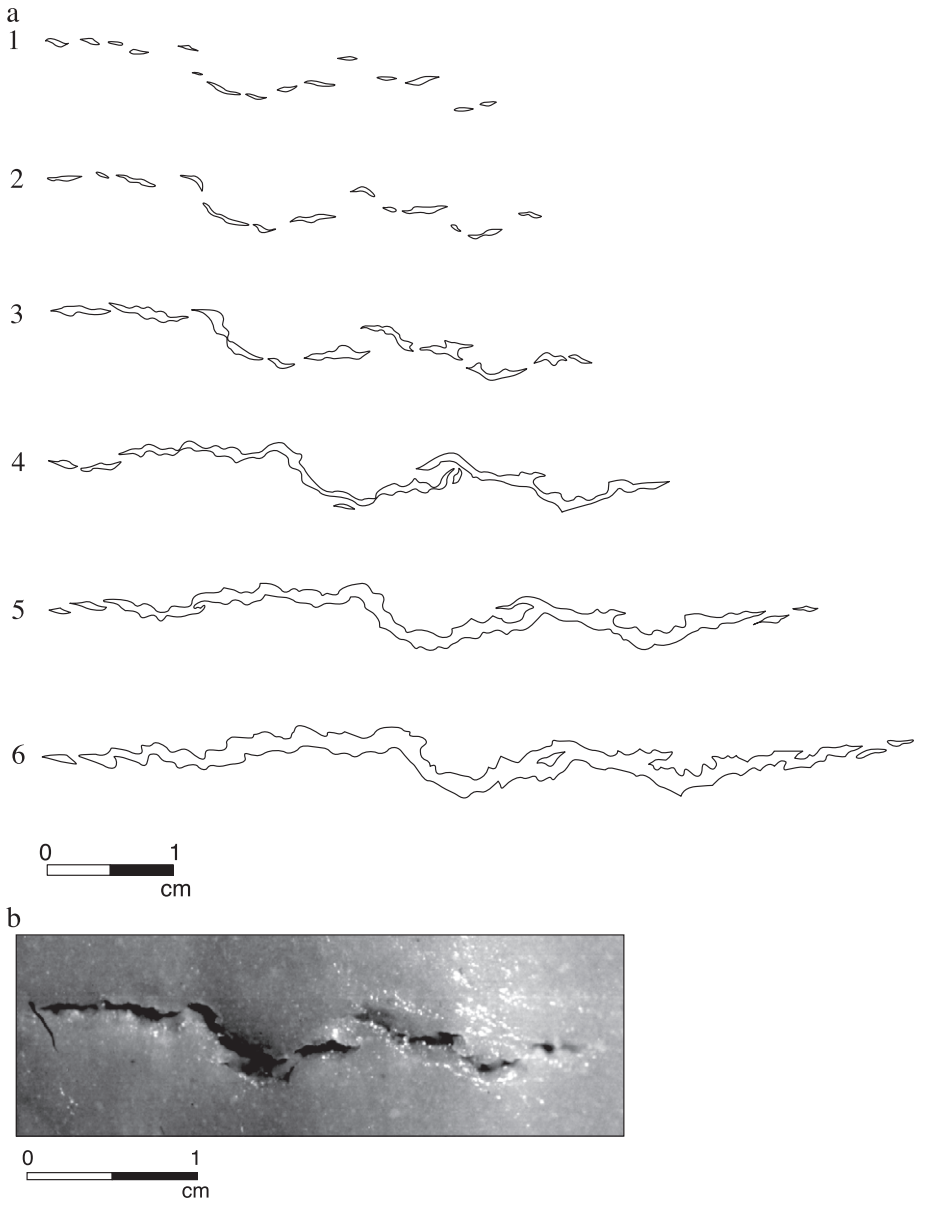

Fig. 2. Initiation and propagation of tension fractures in the model brittle crust, plane view of the model surface. (a) Successive stages (1 to 6) of tension fractures development, drawings from the photographs. (b) Photo of model surface with the fracture pattern at stage intermediate between 3 and 4 above.

putty simulating the lithospheric mantle and asthenosphere. A smaller parallelepiped of weak buoyant material imitating the asthenosphere (or anomalous mantle) was embedded in the stiffer, denser putty simulating the normal mantle (Fig. 1c). Such a starting configuration localizes the diapiric uplift of analogue asthenosphere. The planar layer of semi-brittle material was added to the top of the model as an analogue of the brittle crust. The model was then placed in a centrifuge box with the top surface and two opposing sides free. The space between the model and two of the walls of the centrifuge box permitted uniaxial lateral spreading of the model crust in two opposite directions. The centrifuge run was interrupted at equal time intervals (2–3 min) during the experiment so that fracture propagation and linkage could be photographed on the model's top surface. After each experiment, the deformed model was sectioned to compare the deformation pattern on the free upper surface with its inner parts.

4. Results

4.1. Fracture initiation and propagation

The deformation of the brittle-ductile model was controlled by diapiric uprise of the buoyant analogous asthenospheric material induced by the centrifugal body force (Fig. 1e). This linear upwelling thinned

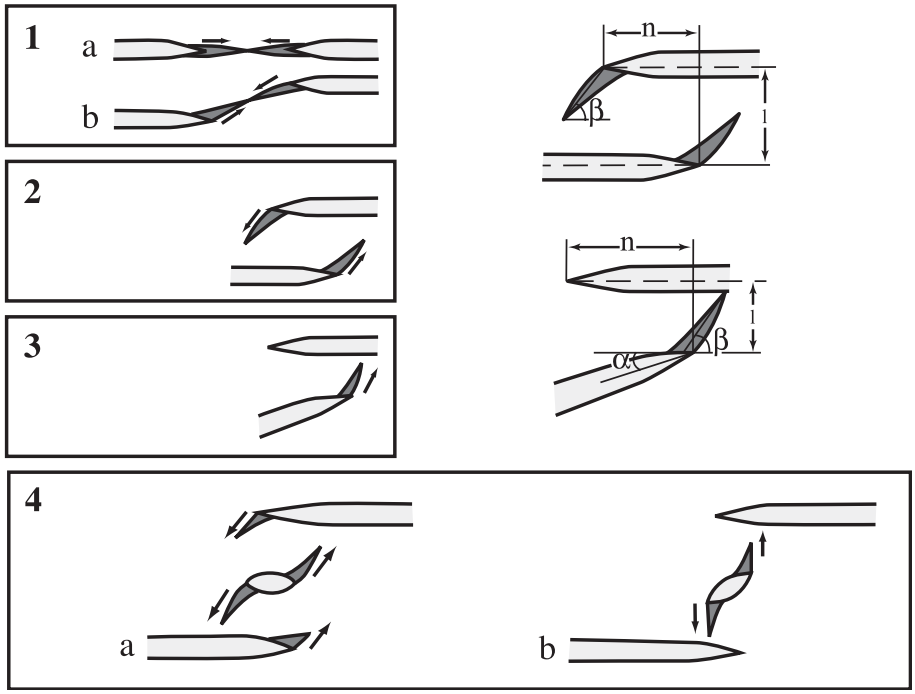

Fig. 3. Types of coalescence patterns between existing (pale) and newly formed (dark) fractures: (1) Tip-to-tip coalescence. Sub-parallel, non-overlapping fractures with small offsets propagate towards each other and coalesce to form a single linear (a) or near-linear (b) fracture. (2) Two-tips-to-two-sidewalls coalescence. Sub-parallel fractures with small overlap and relatively small offset coalesce by tips of each fracture propagating to the sidewall of the other along curved, hook-like paths. (3) One tip-to-one-sidewall coalescence. Fractures that trend at relatively high angles to each other and overlap significantly, coalesce by the tip of one fracture propagating to the sidewall of the other. (4) Third-fracture-nucleation coalescence. When two parallel overlapping fractures have a large offset, a third fracture nucleates within the intervening zone. This third fracture may be parallel or oblique to the overlapping fractures. When parallel (a), the tips of the third fracture propagate toward the opposing sidewalls of the overlapping fractures while the tips of the overlapping fractures propagate towards it. When oblique (b), the tips of the third fracture propagate towards opposing sidewalls of the overlapping fractures, the tips of which do not propagate. Inset: geometric factors of fracture coalescence pattern measured: l—overstep distance between fractures; n—overlap distance between fractures; α—inclination of fracture; β—inclination of secondary fracture.

and displaced the model mantle and induced brittle failure in the upper layer. Fractures in the upper layer occur above local uplifts of analogue asthenosphere. Ductile stretching of analogue mantle in turn allows further upwelling of the diapiric wall of analogue asthenosphere which accelerates lateral extension in the upper layer. The diapir of asthenosphere-like material eventually spreads laterally beneath the brittle layer (Fig. 1f). Strain concentration increases in the brittle layer throughout the rise and spread of the diapir and leads to further fracturing of analogue brittle crust. This surface fracturing in turn affects the top of the diapiric body which intrudes the fractures.

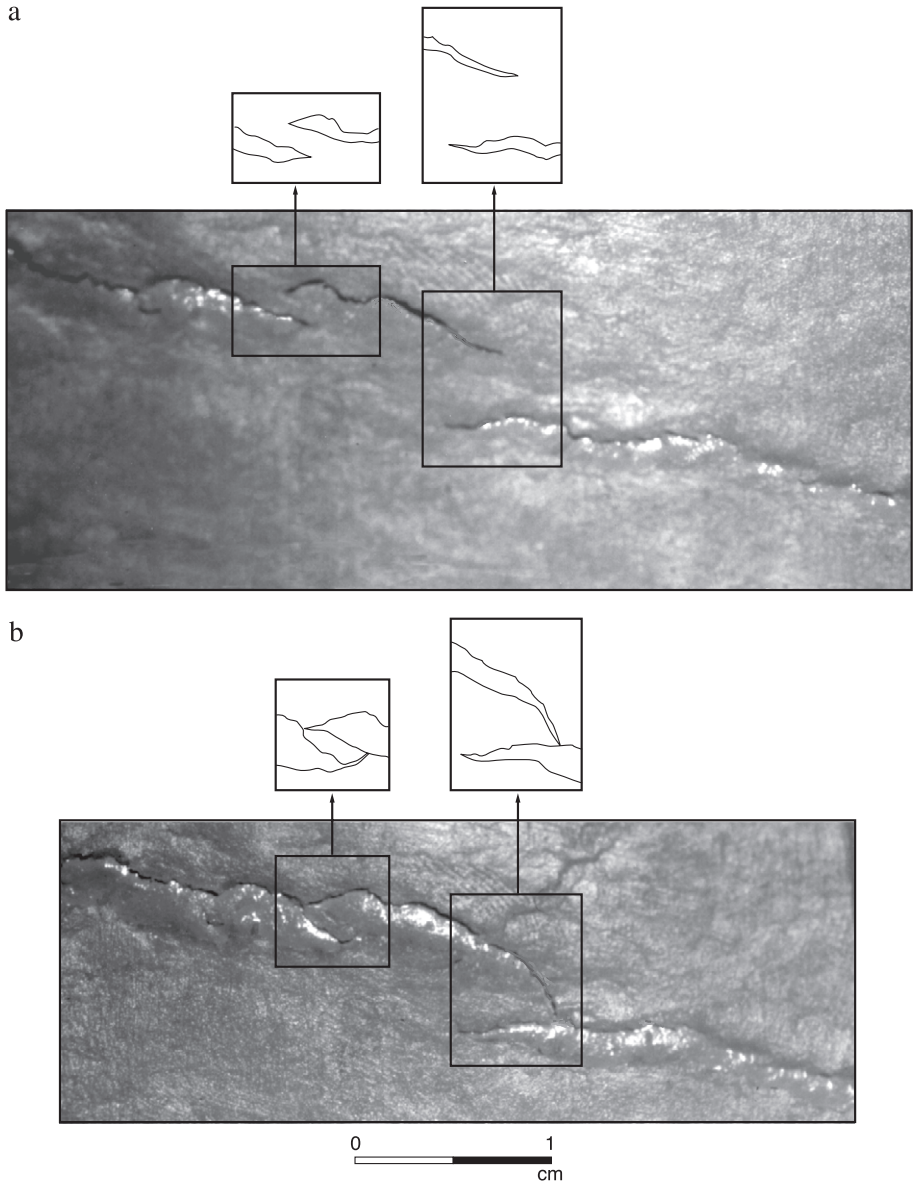

Fig. 4. Photographs of examples of (a) moderate and (b) advanced stages of fracture coalescence of types 2 and 3. Line drawings emphasize coalescence patterns and their evolution. Type 2 fracture coalescence develops on left and type 3 on right.

Initial fractures in the semi-brittle layer are short and sub-parallel but offset (Fig. 2a). As deformation proceeds, the initial cracks propagate longitudinally, coalesce (Fig. 2b) and eventually mature to longer fractures crosscutting the model surface (Fig. 2a, last stages). Few fractures propagate in their own plane. Instead, propagation usually occurs by the joining of new tension cracks initiated beyond the ends of pre-existing fractures. Fracture patterns in the models develop by different types of coalescence between propagating fracture tips. At an advanced stage of fracture development, a single long irregular fracture is usually formed surrounded by small cracks that cease to propagate. Many smaller fractures beside a long fracture remain short because they fail to develop.

4.2. Fracture interaction

The interaction between two fractures is complex and depends on numerous factors. The main purpose of these experiments was to study how the geometry of earlier formed fractures influences their subsequent coalescence. The mode of fracture coalescence was related to measurements in photographs of successive stages in a number of experiments of the following parameters (Fig. 3, inset): (1) the fracture offset distance (l); (2) their overlap distance (n)—which can be positive or negative; (3) their mutual angle of inclination (α) defining their relative trend; and (4) the angle between new propagating fracture and existing portion of other fracture (β). Four main geometric patterns of fracture coalescence were identified in the experiments.

1. Tip-to-tip coalescence.
   Parallel or sub-parallel, non-overlapping fractures with small offsets propagate towards each other and coalesce to form a single linear or near-linear fracture (Fig. 3.1.a and b).
2. Two-tips-to-two-sidewalls coalescence.
   Parallel and sub-parallel fractures with small overlap and offset coalesce by the tips of each fracture propagating to the sidewall of the other along curved, hook-like paths which enclose an elliptical zone between them (Fig. 3.2).

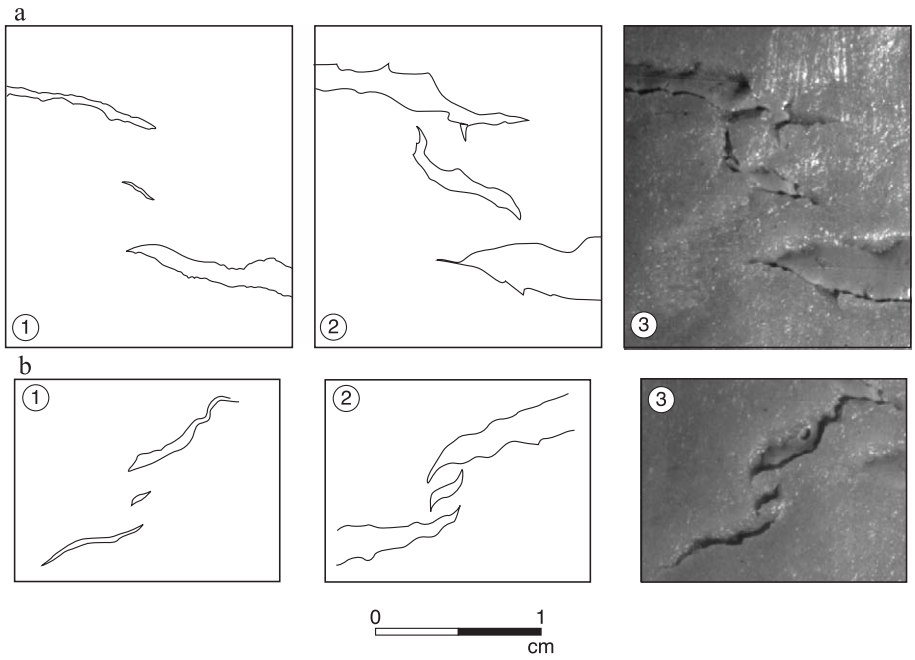

Fig. 5. Drawings and photographs of different stages of fracture coalescence of type 4. Fracture pairs do not coalesce directly but a third fracture nucleates in between them. (a) Third fracture propagates to the sidewalls of existing fractures. (b) Third fracture propagates to the sidewalls of the existing fractures, tips of which also propagate toward third fracture in between them. (1) Moderate stages of extension; (2–3) advanced stages of extension.

3. One tip-to-one-sidewall coalescence.
   Fractures that trend at relatively high angles to each other and overlap significantly coalesce by the tip of one fracture propagating to the sidewall of the other. The fracture at the lower angle to the direction of extension tends to propagate towards the fracture trending at a higher angle to the direction of extension. The fracture at the higher angle to the direction of extension does not propagate (Fig. 3.3).
4. Third-fracture-nucleation coalescence.
   When two parallel overlapping fractures have a large offset, a third fracture nucleates within the overlap zone between them. This third fracture may be parallel or oblique to the overlapping fractures. When parallel (Fig. 3.4.a), the tips of the third fracture propagate towards opposing sidewalls of the overlapping fractures while the overlapping fracture tips propagate towards it. When the third fracture is oblique (Fig. 3.4.b), its tips propagate towards opposing sidewalls of the overlapping fractures while the overlapping fracture tips do not propagate.

In the first group (type 1) of fracture coalescence, the two fractures do not always propagate towards each other at equal rates. The velocity of individual tip propagation depends on the microscopic heterogeneities in the analogue brittle crust. Fracture coalescences of type 2 (Fig. 3.2) and type 3 (Fig. 3.3) are distinguished by whether one or both tips have propagated to a nearby sidewall. Examples of such coalescence are shown in Fig. 4 where a coalescence pattern of group 2 can be seen on the left of the photograph and a group 3 pattern occurs on the right. The propagation paths followed by both tips toward both sidewalls in type 2 coalescence are curved and have relatively low inclination angles (β). By contrast, the propagation paths followed by the single tip towards a single sidewall in type 3 coalescence are straighter with higher inclination (β). Fracture coalescence is more complex in group 4 patterns (Fig. 3.4).

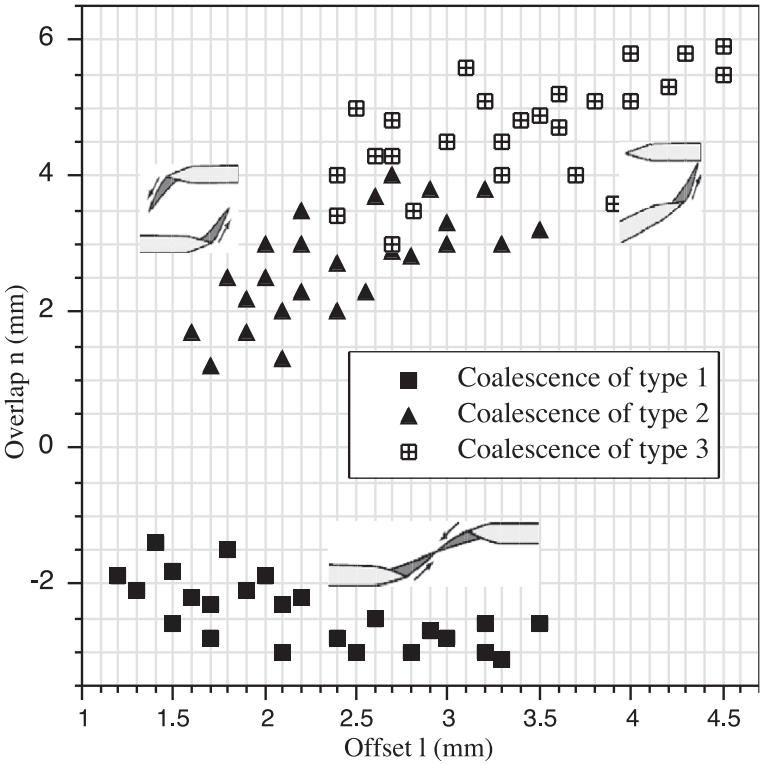

Fig. 6. Types of fracture coalescence patterns distinguished on a plot of their offset (l) against overlap (n).

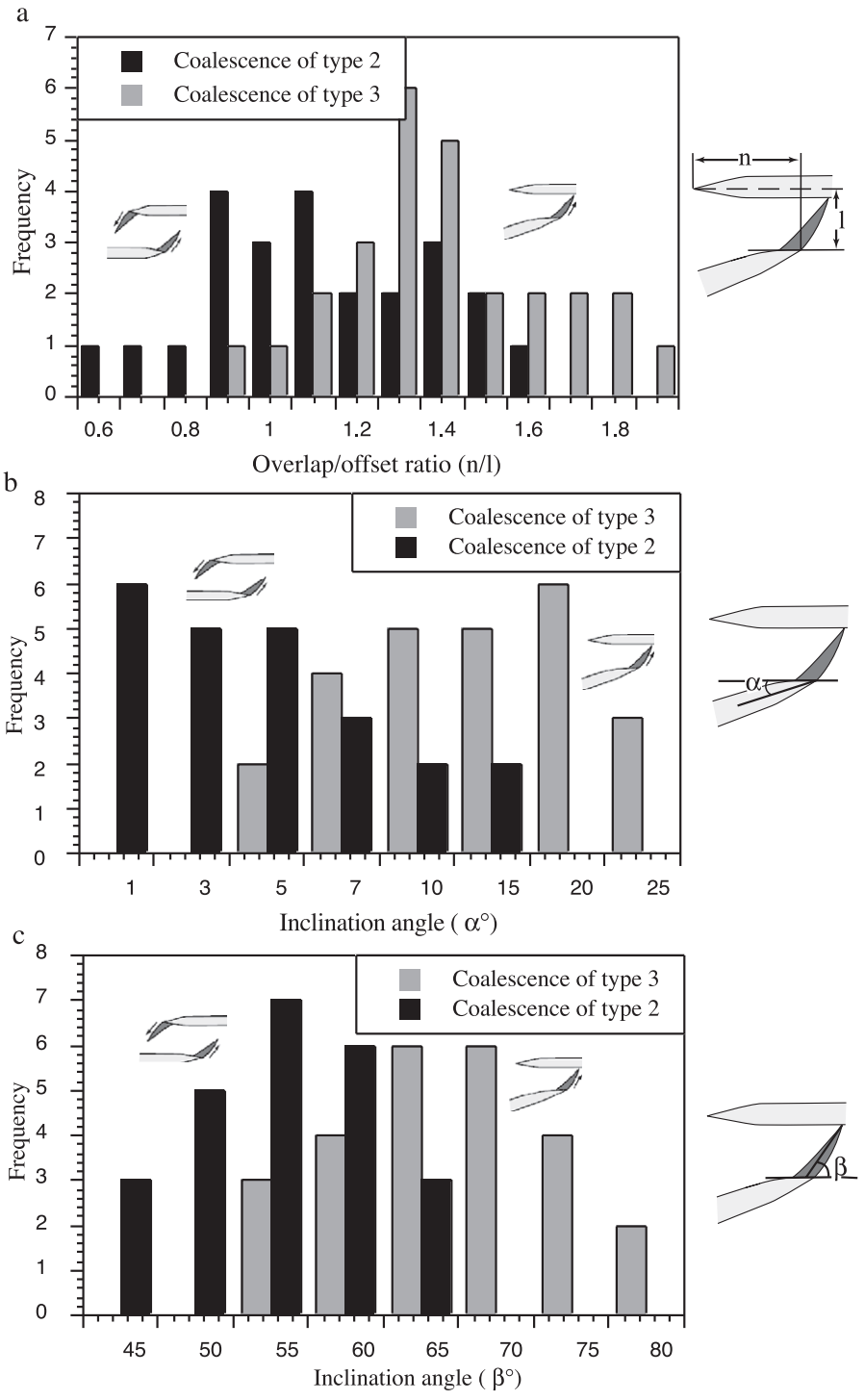
a
Coalescence of type 2
Coalescence of type 3
Frequency
Overlap/offset ratio (n/l)
n
l
b
Coalescence of type 3
Coalescence of type 2
Frequency
Inclination angle (α°)
α
c
Coalescence of type 3
Coalescence of type 2
Frequency
Inclination angle (β°)
β

The trend of the third fracture developed between overlapping pre-existing fractures appears to define whether case 4a or 4b occurs for most fracture pairs. Examples of group 4 coalescence are shown in Fig. 5. Type 4 coalescence appears to develop as a combination of type 2 or type 3 fracture interaction. Therefore, type 4 coalescence will not be analyzed further here and other fracture patterns will be considered in more detail.

Fig. 6 shows how different types of fracture coalescence relate to overlap and offset distances. As the thickness of the fracturing layer was 1 mm in all models, offsets and overlaps measured in millimeters can be considered as normalized to the layer thickness. The value of offset is generally low for type 1 coalescence (1.2–3.5 mm). Comparison of the other two modes of fracture interaction shows that fracture pairs of type 3 coalescence have a slightly wider range of values for offset (2.4–4.5 mm) compared to type 2 (1.6–3.5 mm, mainly 1.9–3 mm). The values of overlap distance are a distinctive characteristic of the mode of fracture interaction. Coalescence of type 1 takes place where fracture pairs have negative overlap, coalescence of type 2 occurs where positive overlaps are small (1–4 mm), whereas type 3 coalescence preferably develops between fractures with large positive overlap (3–6 mm). Thus the overlaps of the fracture pairs in Fig. 4 differ for group 2 and group 3 coalescence: the overlap on the right part of the photograph is about 1.5 times larger than that on the left. The ratio n/l also distinguishes types 2 and 3 coalescence (Fig. 7a), being between 0.6 and 1.6 for type 2 and between 0.9 and 1.9 for type 3. The threshold conditions for fracture overlap and offset that mark the transition between coalescence of different types can be defined as follows: $n = 0$ for transition between types 1 and 2 + 3 and $n/l = 1.2 \pm 0.3$ for the transition between types 2 and 3.

Fig. 7b shows how the trend of fractures controls their coalescence. Type 2 coalescence tends to develop between fracture pairs with low inclination angles ($\alpha = 1–15°$, mainly 1–5°), while coalescence of type 3 is more usual where inclinations are higher ($\alpha = 4–25°$, mainly 10–20°). The pair of fractures to the left in Fig. 4 are sub-parallel, whereas the fracture pair to the right in Fig. 4 trend obliquely at a mutual inclination of $\alpha = 18°$. The transition between coalescence of types 2 and 3 as defined by inclination angle appears to be rather smooth: $4° < \alpha < 15°$.

The trend of the younger fractures differs in the fracture pairs of groups 2 and 3. Fig. 7c shows how the inclination of the secondary fracture (β) controls their coalescence. The inclination angle of the secondary fracture (β) in group 2 generally vary between 45° and 65°, and in group 3 between 50° and 80°. The threshold conditions between coalescence of types 2 and 3 appear as: $54° < \beta < 65°$.

5. Discussion

5.1. Fracture initiation

Fractures in the models propagate by the formation of small cracks in regions of high stress concentration near their tips. This is similar to the propagation of micro-cracks to form macro-fractures in natural rocks (Segall and Pollard, 1983; Gudmundsson, 1987), the emplacement of igneous dikes (Delaney et al., 1986), and the development of micro-cracks in rock specimens subject to loading (Kobayashi and Fourney, 1978). Each fracture begins to grow when a local propagation condition is met (Segall and Pollard, 1983).

Two explanations have been offered for the early development of coplanar but offset fractures. Lawn and Wilshaw (1975) suggested that a single propagating fracture splits into several nearly parallel fractures because of local stress anomalies developed in its advancing tip zone. By contrast, Gudmundsson (1987) attributed the simultaneous development of multiple offset coplanar fractures to failure occurring wherever the resolved tensile stress exceeds the tensile strength of the failing material. Gudmundsson's

Fig. 7. (a) The characteristic overlap/offset ratio for fracture pairs with coalescence of types 2 and 3. The values of measured n/l ratios are plotted against the numbers of offsets studied. (b) Types 2 and 3 fracture coalescence patterns distinguished on a plot of the angle of inclination (α) between pairs of fractures plotted against the frequency (number) of cases. (c) Types 2 and 3 fracture coalescence patterns distinguished on a plot of the angle of inclination (β) of paths followed by propagating fracture tips. Inclination of secondary fracture (β) plotted against the frequency (number) of cases.

(1987) picture is obviously more appropriate for the simultaneous development of multiple offset coplanar fractures in the brittle top layer of the models described here.

The primary causes of fracture formation on the ocean floor are believed to be associated with the build-up of regional stress, due to plate movements (e.g. gravity gliding) and dyke intrusions directed by magmatic pressure related to overall asthenospheric uplift. The sites of ridge segments and their trends on the ocean floor are controlled grossly by the regional stress field. However, the location of each individual ridge segment may also depend on rheological heterogeneities in the crust and mantle. In the models described here, extension of the brittle layer is focussed by the diapiric body rising from below, but is not uniformly distributed. ''Ridge jump'' occurs when a new offset fracture nucleates as a result of the stresses exceeding the tensile strength of the brittle layer at a new site of weakness (Shemenda and Grocholsky, 1994). Such fracture initiation in nature is believed to be controlled by the rheological state and geometry of the crustal and mantle units and their boundaries. As in the models by Shemenda and Grocholsky (1994), in the present experiments, various types of transfer/accommodation zones were generated between adjacent segments of the spreading axis. As each model evolves, the number of individual fractures increases. This results in a complex interacting system of fractures but the pattern in the ''axial rift zone'' simplifies somewhat when short fractures link to form a single continuous fracture.

5.2. Fracture propagation

This work attempted to study formation of overlap zones between interacting fractures as analogues of ridge segments. In the models the average of overlap/offset ratio $n/l = 1.2$. It should be emphasized that this ratio characterizes geometry of a pair of interacting fractures prior to formation of the overlap zone. It cannot be directly compared to dimensions of existing OSCs on oceanic floor that usually exhibit length/width ratios of about 2.1 to 3:1 (Macdonald et al., 1984; Sempere and Macdonald, 1986). If configuration of produced overlap zones in the present models should be considered, it would generally satisfy the dimensions of oceanic OSCs.

Each of the present models was constructed in an attempt to study the evolution of ridge segments at the conditions of continuous spreading. While it was generally accepted that instability of spreading direction results in the formation of more complex pattern of structures on the ocean floor, there were debates on whether or not it should be considered as a primary origin for the formation of rift-zone OSCs. Macdonald et al. (1984) and Macdonald (1988) suggested that a change in the direction of spreading might lead to a preferred sense of offset of groups of OSCs, but was not a necessary condition for OSCs development. Lonsdale (1985, 1986) argued that OSCs ultimately result from a change in the relative motion of the accreting plates. In all experiments presented here, constant orientation of maximum tensile stress always resulted in stability of spreading direction. The appearance of overlapping fractures in the models, therefore, suggests that formation of OSCs does not necessary result from the change in the spreading direction.

In the experiments described here, fractures in the brittle layer widen at the same time as they propagate laterally. Analogue mantle wells up in each dilational fracture which thus acts as a local spreading centre. After moderate extension, long fractures tend to develop at the expense of short ones. Long fractures develop when fracture initiation is progressive (Rives et al., 1994). Parker (1981) defines the crack extension force of strain energy release rate per crack tip, G, for plane stress as: $G = dU/da = \pi\vartheta^2 aE^{-1}$. Here, U is the elastic energy released per unit thickness of rock due to crack propagation, a is the half-length of the crack, ϑ is the applied external tensile stress (or internal fluid pressure) and E is the Young's modulus of the rock. This equation shows that, if ϑ is constant, G increases linearly with increasing crack length, so that long fractures are more likely to propagate. The model of Macdonald et al. (1991) emphasizes that in a mechanism for ridge segment lengthening, the crack propagation force caused by far-field plate stresses plays the dominant role, while considering the stress intensity factors associated with far-field stresses together with gravitational spreading forces to be additive.

5.3. Fracture interaction

We have tested experimentally the relative importance of the distance between fractures, their overlap,

and their trends, in controlling the maturation of fracture patterns simulating the propagation of the mid-ocean ridges. The overlap distances between fractures and their relative trends control whether they will continue to propagate parallel to their trend or curve toward each other. Type 1 coalescence, where cracks lengthen by joining each other end-to-end, should be rather common. However, once cracks have joined end-to-end, there remains little evidence of this transient state. In addition, type 1 coalescence obscures any preceding offset so that it is difficult to determine the location of earlier crack tips.

Fracture overlaps and the relative orientations of fracture pairs define whether one or two fracture tips propagate to coalescence and, in addition, influence the degree of fracture curvature. In the case of type 2 coalescence (Fig. 3.2; Fig. 4, left), stress concentration near each of the tips results in the formation of hook-shaped fractures, structures reminiscent of larger-scale patterns described as OSCs on the seafloor (Macdonald, 1988). Local shear stresses due to crack interaction cause fracture propagation paths to curve (Pollard et al., 1982; Tuckwell et al., 1998). The propagation path of each fracture tip is influenced by the local stress-field around the other tip, causing both fracture paths to curve toward each other. Fracture linkage occurs as a result of the close interaction of stress-fields ahead of the propagating fracture tips. However, often two neighboring interacting fractures do not coalesce, with their tips remaining curved, isolated. Macdonald et al. (1987) have shown that it occurs because as fractures grow and overlap, the crack propagation force can drop to less than that for an isolate crack depending on the configuration of the produced overlap. For those fracture pairs that have eventually linked during the course of the experiment, the enclosure and later rotation of intact blocks between overlapping individual hook-like fractures is similar to the rotation of the basins between the arms of many overlapping spreading centers proposed in a number of studies (Macdonald and Fox, 1983; Macdonald et al., 1984; Macdonald, 1988) and observed on the seafloor (Carbotte and Macdonald, 1992; Perram et al., 1993; Bird and Naar, 1994). This type of fracture interaction is common in nature on a large range of scales. Examples of this type of coalescence are observed in tension fractures in Holocene basaltic lava flows in a large number of locations in Iceland subject to extension along the active rift zone (Fig. 8a). The aerial view demonstrates a pair of overlapping fractures in which both tips propagated along curved paths. Study of ocean floor structures reveals similar geometries for OSCs. Fig. 9a shows bathymetric images of parts of the Northeast Pacific ridges (Ryan et al., 2001) indicating that lateral interaction of these ridge segments involved two-tips-to-two-sidewalls propagation.

In type 3 coalescence patterns, where linkage involves the propagation of only one fracture tip to the sidewall of another (Fig. 3.3; Fig. 4, right),

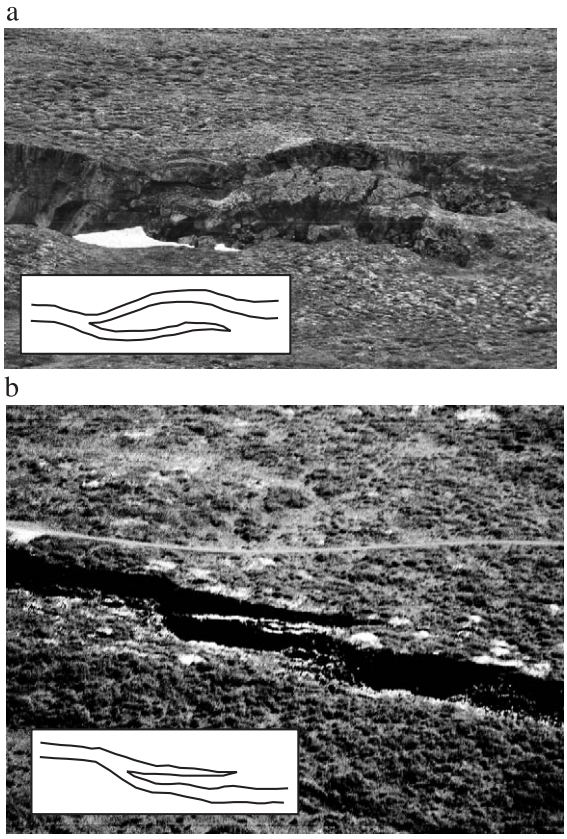

Fig. 8. Fractures in basaltic Holocene lava in Iceland. (a) Partial coalescence is apparently produced by curved propagation of both fracture tips and corresponds to type 2. The photograph is taken from an airplane at Gjastykki, Myvatn area, northeastern Iceland. (b) Coalescence apparently involved propagation of a single fracture tip and corresponds to type 3. Oblique air photograph taken from the air of the area of the Thinvellir fissure swarm, southwestern Iceland.

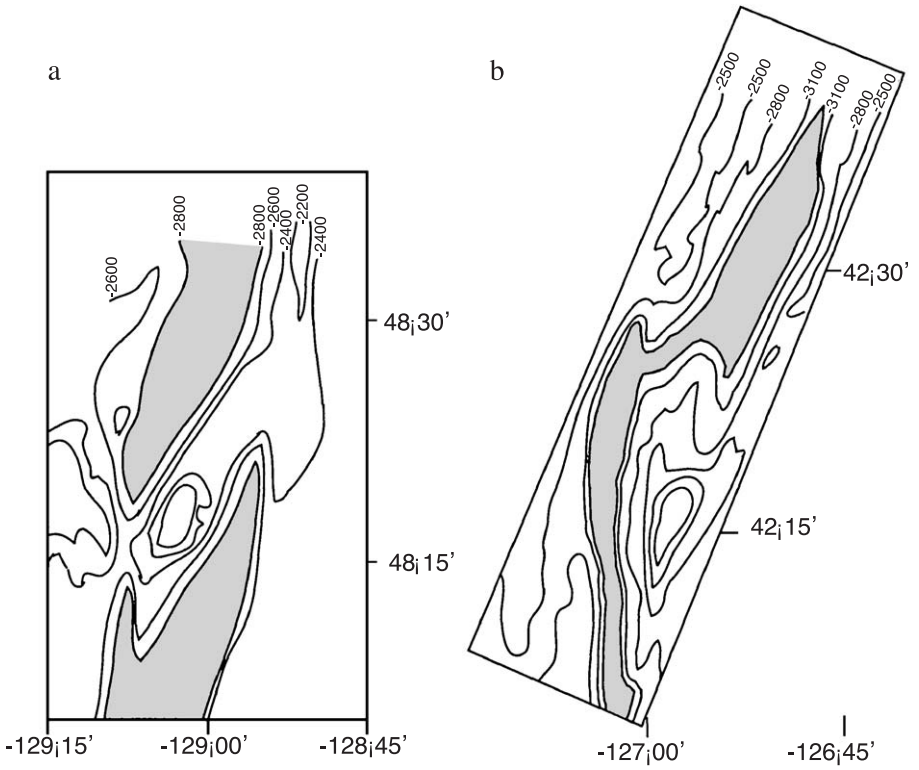

Fig. 9. Bathimetry images of parts of the Northeast Pacific ridges (modified from Ryan et al., 2001). Two types of fracture coalescence identified in analogue models can be distinguished in these ridge segments. (a) Coalescence of type 2 (two-tips-to-two-sidewalls propagation). Labeled contours are at 200-m intervals. Elevation in meters is indicated above sketch. Area deeper than 2800 m is shaded to emphasize geometry of segments. (b) Coalescence of type 3 (one tip-to-one-sidewall propagation). Labeled contours are at 300-m intervals. Area within ridge deeper than 3400 m is shaded.

stresses around the tip of the other fracture are relaxed and it ceases to propagate. As a crack tip propagates, the path it follows becomes progressively parallel to the spreading direction. Tuckwell et al. (1998) attributed this effect to the zone around the propagating fracture tip being increasingly affected by the wall of the fracture it is approaching. It appears that if two spreading segments in the present model link by a fracture striking close to parallel with the spreading direction, this fracture is most likely to nucleate at the end of the segment propagating in the overlap zone. This agrees with the observations of Oldenburg and Brune (1975) on orthogonal fractures in paraffin wax. Coalescence induces local shear stress along the tip of the fracture propagating close to the spreading direction, so that it becomes capable of accommodating lateral motion. This state of stress is similar to that which characterizes transform fault zones in oceanic rift systems (Fox and Gallo, 1984; Bird and Naar, 1994; Taylor et al., 1994) and in Iceland (Young et al., 1985; Gudmundsson, 1995; Rögnvaldsson et al., 1998; Gudmundsson and Homberg, 1999). It is also similar to strike-slip fault zones simulated in analogue models (Mauduit and Dauteuil, 1996; Dauteuil and Mart, 1998; Acocella et al., 1999). Thus the development of extreme examples of type 3 coalescence (β>70°) may be important in the initiation of those transform faults not inherited from continental break-up. The field example of type 3 fracture interaction in Holocene basaltic rocks of the axial rift zone in Iceland is shown in Fig. 8b. An aerial view shows fracture pairs where coalescence involved only one

fracture propagating to the wall of the other. A similar pattern is recognizable on the ocean floor where mid-ocean ridge segments interact. Thus, lateral linkage of segments of Northeast Pacific ridges in Fig. 9b (after Ryan et al., 2001) can be inferred to have involved one tip-to-one-sidewall propagation.

5.4. Summary

The results of modeling described here are considered relevant to the processes controlling fracture growth in the brittle crust in general. Extension at the Earth's surface is mostly accommodated by tension fracture systems (Gudmundsson, 1991, 2000). Direct observations of how fracture patterns develop in models should improve the understanding of the basic factors that control fracture initiation, propagation and coalescence.

The experiments described here modeled the spontaneous evolution of fracture swarms developing in a thin semi-brittle layer on the top of the analogue mantle laterally stretched by an upwelling diapiric body of the analogue asthenosphere driven by a centrifugal force modeling gravity. Offset subparallel fractures initiate simultaneously in the model crust at sites of microscopic weaknesses within a zone of high tensile stress overlying the upwelling diapiric body. Sub-vertical fractures propagate perpendicular to the maximum tensile stress by coalescence of small tension cracks initiated in the vicinities of their tips. In the models, there are a limited number of ways in which individual fractures link. We have outlined distinct geometries of coalescence between pairs of fractures, involving tip-to-tip and tip-to-sidewall interactions. These types can be differentiated by comparison of key parameters, including the fracture offset and overlap distances and their relative trend.

6. Conclusions

1. The direction of maximum extensional stress at each individual fracture tip is affected by nearby fractures.
2. The coalescence of maturing fractures depends on the geometries of interacting fracture pairs. Their modes of propagation depend on their offset, overlap and trend.
3. Coalescence patterns of type 2 are characterized by curved paths where each fracture propagates to the sidewall of the other enclosing an elliptical zone between them. Stress concentration near each of the tips results in the formation of the hook-shaped structures reminiscent of patterns described on larger scales associated with OSCs on the seafloor.
4. In type 3 coalescence, as one fracture tip propagates, its path becomes progressively parallel to the spreading direction to meet the sidewall of a non-propagating adjacent fracture. Coalescence involves local shear stress around the propagating fracture tip, as in zones of high-shear stress documented along oceanic transform faults.
5. Evolving patterns of individual fractures observed in the dynamically scaled analogue models described here can be applied to large-scale fractures in rocks in extensional areas, to segments of mid-ocean ridges, and the coalescence of segments associated with different spreading centers on the ocean floor.

Acknowledgements

I would like to thank Dr. Mulugeta for valuable advice on the choice of modeling materials and experimental set-up as well as supervision during the work. General support and repeated revisions of the manuscript by Dr. Talbot are greatly appreciated. Finally, I am grateful to Dr. Macdonald and Dr. Sloan for the thoughtful comments and support.

References

Acocella, V., Faccenna, C., Funiciello, R., Rossetti, F., 1999. Sandbox modelling of basement-controlled transfer zones in extensional domains. Terra Nova 11, 149–156.

Angelier, J., Bergerat, F., Dauteuil, O., Villemin, T., 1997. Effective tension-shear relationships in extensional fissure swarms, axial rift zone of northeastern Iceland. J. Struct. Geol. 5, 673–685.

Bird, R.T., Naar, D.F., 1994. Intratransform origins of mid-ocean ridge microplates. Geology 22, 987–990.

Carbotte, S.M., Macdonald, K.C., 1992. East Pacific Rise 8°–

10°30′N: evolution of ridge segments and discontinuities from SeaMARC II and three-dimensional magnetic studies. J. Geophys. Res. 97, 6959–6982.
Cotterell, B., Rice, J.R., 1980. Slightly curved or kinked cracks. Int. J. Fract. 16, 155–169.
Cowie, P.A., 1998. Normal fault growth in three-dimensions in continental and oceanic crust. Faulting and Magmatism at Mid-Ocean Ridges. American Geophysical Union, Washington, DC, pp. 325–348.
Cowie, P.A., Scholz, C.H., Edwards, M., Malinverno, A., 1993. Fault strain and seismic coupling on mid-ocean ridges. J. Struct. Geol. 98, 17911–17920.
Dauteuil, O., Mart, Y., 1998. Analogue modeling of faulting pattern, ductile deformation, and vertical motion in strike-slip fault zones. Tectonics 17, 303–310.
Davies, G.F., 1999. Dynamic Earth. Cambridge Univ. Press, Cambridge. 457 pp.
De Bremaecker, J.Cl., Swenson, D.V., 1990. Origin of overlapping spreading centers: a finite element model. Tectonics 9, 505–519.
Delaney, P.T., Pollard, D.D., Ziony, J.I., McKee, E.H., 1986. Field relations between dikes and joints: emplacement processes and paleostress analysis. J. Geophys. Res. 91, 4920–4938.
Fowler, C.M.R., 1990. The Solid Earth: An Introduction to Global Geophysics. Cambridge Univ. Press, Cambridge. 472 pp.
Fox, P.J., Gallo, D.G., 1984. A tectonic model for ridge-transform–ridge plate boundaries: implications for the structure of oceanic lithosphere. Tectonophysics 104, 205–242.
Goodman, R.E., 1989. Introduction to Rock Mechanics. Wiley, New York. 562 pp.
Gudmundsson, A., 1987. Tectonics of the Thingvellir fissure swarm, SW Iceland. J. Struct. Geol. 1, 61–69.
Gudmundsson, A., 1991. Structure and development of the Svenagja graben, Northeast Iceland. Tectonophysics 200, 111–125.
Gudmundsson, A., 1993. Structural analysis of a transform fault–rift zone junction in North Iceland. Tectonophysics 220, 205–221.
Gudmundsson, A., 1995. Stress fields associated with oceanic transform faults. Earth Planet. Sci. Lett. 136, 603–614.
Gudmundsson, A., 2000. Dynamics of volcanic systems in Iceland: example of tectonism and volcanism at juxtaposed hot spot and mid-ocean ridge systems. Annu. Rev. Earth Planet Sci. 28, 107–140.
Gudmundsson, A., Homberg, C., 1999. Evolution of stress fields and faulting in Seismic zones. Pure Appl. Geophys. 154, 257–280.
Jaeger, J.C., Cook, N.G.W., 1979. Fundamentals of Rock Mechanics. Chapman & Hall, London. 593 pp.
Kobayashi, T., Fourney, W.L., 1978. Experimental characterization of the development of the micro-crack process zone at a crack tip in rock under load. In: Kim, Y.S. (Ed.), 19th U.S. Symposium on Rock Mechanics, vol. 1. University of Nevada-Reno, Reno, NV, pp. 243–246.
Krasnov, S., Poroshina, I., Cherkashev, S., Mikhalsky, E., Maslov, M., 1997. Morphotectonics, volcanism and hydrothermal activity on the East Pacific Rise between 21°12′S and 22°40′S. Mar. Geophys. Res. 19, 287–317.
Lawn, B.R., Wilshaw, T.R., 1975. Fracture of Brittle Solids. Cambridge Univ. Press, Cambridge. 204 pp.
Lonsdale, P., 1983. Overlapping rift zones at the 5.5°S offset of the East Pacific Rise. J. Geophys. Res. 88, 9393–9406.
Lonsdale, P., 1985. Nontransform offsets of the Pacific-Cocos plate and their traces on the rise flank. Geol. Soc. Amer. Bull. 96, 313–327.
Lonsdale, P., 1986. Comments on "East Pacific Rise Siqueiros to Orozco Fracture Zones: along-strike continuity of axial neovolcanic zone and structure and evolution of overlapping spreading centres" By K. Macdonald, J. Sempere and P.J. Fox. J. Geophys. Res. 91 (B10), 10493–10499.
Macdonald, K.C., 1986. The crest of the Mid-Atlantic Ridge: models for crustal generation processes and tectonics. In: Vogt, P.R., Tucholke, B.E. (Eds.), The Geology of North America. The Western North Atlantic Region, Vol. M. The Geological Society of America, Boulder, CO, pp. 51–66.
Macdonald, K.C., 1988. A new view of the mid-ocean ridge from the behaviour of ridge-axis discontinuities. Nature 335, 217–225.
Macdonald, K.C., 1998. Linkages between faulting, volcanism, hydrothermal activity and segmentation on fast spreading centres. In: Faulting and Magmatism at Mid-Ocean Ridges. American Geophysical Union, Washington, DC, pp. 27–58.
Macdonald, K.C., Fox, P.J., 1983. Overlapping spreading centres: a new kind of accretion geometry on the East Pacific Rise. Nature 302, 55–58.
Macdonald, K.C., Sempere, J.-C., Fox, P.J., 1984. East Pacific rise from Siqueiros to Orozco fracture zones: along-strike continuity of axial neovolcanic zone and structure and evolution of overlapping spreading centres. J. Geophys. Res. 89, 6049–6069.
Macdonald, K.C., Sempere, J.-C., Fox, P.J., Tyce, R., 1987. Tectonic evolution of ridge axis discontinuities by the meeting, linking, or self-decapitation of neighboring ridge segments. Geology 15, 993–997.
Macdonald, K.C., Scheirer, D.S., Carbotte, S.M., 1991. Mid-ocean ridges: discontinuities, segments and giant cracks. Science 253, 986–994.
Mauduit, T., Dauteuil, O., 1996. Small-scale models of oceanic transform zones. J. Geophys. Res. 98, 12251–12265.
McAlister, E., Cann, J.R., 1996. Initiation and evolution of boundary wall faults along the Mid-Atlantic Ridge, 25–29°N. In: MacLeod, C.J., Tyler, P.A., Walker, C.L. (Eds.), Tectonic, Magmatic, Hydrothermal and Biological Segmentation at Mid-ocean Ridges. Spec. Publ.-Geol. Soc. Lond., vol. 118, pp. 29–48.
Mulugeta, G., 1988. Squeeze box in a centrifuge. Tectonophysics 148, 323–335.
Oldenburg, D.W., Brune, J.N., 1975. An explanation for the orthogonality of ocean ridges and transform faults. J. Geophys. Res. 80, 2575–2585.
Olson, J., 1993. Joint pattern development: effect of subcritical crack growth and mechanical crack interaction. J. Geophys. Res. 98, 12251–12265.
Olson, J.E., Pollard, D.D., 1989. Inferring paleostresses from natural fracture patterns: a new method. Geology 17, 345–348.
Parker, A.P., 1981. The Mechanics of Fracture and Fatigue. Spon, London. 167 pp.
Perram, L.J., Cormier, M.-H., Macdonald, K.C., 1993. Magnetic and tectonic studies of the dueling propagating spreading cen-

ters at 20°40′S on the East Pacific Rise: evidence for crustal rotations. J. Geophys. Res. 98, 13835–13850.
Pollard, D.D., Aydin, A., 1984. Propagation and linkage of oceanic ridge segments. J. Geophys. Res. 89, 10017–10029.
Pollard, D.D., Segall, P., Delaney, P.T., 1982. Formation and interpretation of dilatant cracks. Geol. Soc. Amer. Bull. 3, 1291–1303.
Ramberg, H., 1981. Gravity, Deformation and the Earth's Crust. Academic Press, London. 452 pp.
Ranalli, G., 1987. Rheology of the Earth. Allen & Unwin, USA. 366 pp.
Rives, T., Rawnsley, K.D., Petit, J.-P., 1994. Analogue simulation of natural orthogonal joint set formation in brittle varnish. J. Struct. Geol. 16, 419–429.
Rögnvaldsson, S.T., Gudmundsson, A., Slunga, R., 1998. Seismotectonic analysis of the Tjörnes Fracture Zone, an active transform fault in north Iceland. J. Geophys. Res. 103 (B12), 30117–30129.
Ryan, W., Haxby, W., Carbotte, S., O'Hara, S., 2001. RIDGE Multibeam Synthesis Project, http://ocean-ridge.ldeo.columbia.edu/.
Segall, P., Pollard, D.D., 1983. Joint formation of granitic rock of the Sierra Nevada. Geol. Soc. Amer. Bull. 94, 563–575.
Sempere, J.-C., Macdonald, K.C., 1986. Overlapping spreading centers: implications from crack growth simulation by the displacement discontinuity method. Tectonics 5, 151–163.
Shaw, P.R., Lin, J., 1993. Causes and consequences of variations in faulting style at the Mid-Atlantic Ridge. J. Geophys. Res. 98, 21839–21851.
Shemenda, A.I., Grocholsky, A.L., 1991. A formation and evolution of overlapping spreading centers (constrained on the basis of physical modeling). Tectonophysics 199, 398–404.
Shemenda, A.I., Grocholsky, A.L., 1994. Physical modeling of slow seafloor spreading. J. Geophys. Res. 99, 9137–9153.
Shen, B., Stephansson, O., Einstein, H.H., Ghahreman, B., 1995. Coalescence of fractures under shear stresses in experiments. J. Geophys. Res. 100, 5975–5990.
Shih, J., Molnar, P., 1975. Analysis and implications of the sequence of ridge jumps that eliminated the Surveyor transform fault. J. Geophys. Res. 80, 4815–4822.
Solomon, S.C., Huang, P.Y., Meinke, L., 1988. The seismic moment budget of slowly spreading ridges. Nature 334, 58–61.
Taylor, B., Crook, K., Sinton, J., 1994. Extensional transform zones and oblique spreading centers. J. Geophys. Res. 99 (B10), 19707–19718.
Tentler, T., 2001. Experimental study of single layer folding in nonlinear materials. In: Koyi, H.A., Mancktelow, N.S. (Eds.), Tectonic Modeling: A Volume in Honor of Hans Ramberg. Mem. Geol. Soc. Amer., vol. 193, pp. 89–99. Boulder, CO.
Thomas, A.L., Pollard, D.D., 1993. The geometry of echelon fractures in rock: implications from laboratory and numerical experiments. J. Struct. Geol. 15, 323–334.
Tuckwell, G.W., Bull, J.M., Sanderson, D.J., 1998. Numerical models of faulting at oblique spreading centers. J. Geophys. Res. 103, 15473–15482.
Weijermars, R., Schmeling, H., 1986. Scaling of Newtonian and non-Newtonian fluid dynamics without inertia for quantitative modelling of rock flow due to gravity (including the concept of rheological similarity). Phys. Earth Planet. Inter. 43, 316–330.
Young, K.D., Jancin, M., Voight, B., Orkan, N.I., 1985. Transform deformation of Tertiary rocks along the Tjornes fracture zone, North Central Iceland. J. Geophys. Res. 90 (B12), 9986–10010.